

5-2017

# Hydrogen Molybdenum Bronze Catalyzed Hydrolysis of Cellulose

Claire O. Baker

*East Tennessee State University*

Follow this and additional works at: <https://dc.etsu.edu/honors>



Part of the [Analytical Chemistry Commons](#)

---

## Recommended Citation

Baker, Claire O., "Hydrogen Molybdenum Bronze Catalyzed Hydrolysis of Cellulose" (2017). *Undergraduate Honors Theses*. Paper 409.  
<https://dc.etsu.edu/honors/409>

This Honors Thesis - Withheld is brought to you for free and open access by the Student Works at Digital Commons @ East Tennessee State University. It has been accepted for inclusion in Undergraduate Honors Theses by an authorized administrator of Digital Commons @ East Tennessee State University. For more information, please contact [digilib@etsu.edu](mailto:digilib@etsu.edu).

## TABLE OF CONTENTS

Section	Page
1. Abstract.....	2
2. Acknowledgements.....	3
3. List of Tables .....	4
4. List of Figures.....	5
5. List of Schemes.....	6
6. Introduction.....	7
6.1. Need for Biofuels.....	8
6.2. Cellulose as an Energy Source .....	9
6.3. Hydrogen Bronzes for Hydrolysis of Cellulose .....	12
6.4. Total Organic Carbon Determination of Hydrolyzed Cellulose.....	16
7. Experimental.....	20
7.1. Materials and Methods .....	20
7.2. Experimental Procedure.....	20
8. Results and Discussion .....	22
8.1. Calibration of TOC Method.....	22
8.2. Average Absorbances and TOC Concentrations .....	22
9. Conclusions.....	26
10. Future Prospects.....	28
11. References.....	29

## ABSTRACT

In recent years, there has been increasing concern with respect to the large dependence across the globe on nonrenewable energy sources, such as fossil fuels. Ethanol has been explored, however, in alleviating this problem; cellulose, a polymer of glucose molecules, is a precursor to this potentially useful biofuel. However, the strength and rigidity of the cellulose structure has proven to be a difficult obstacle to overcome in this multistep synthesis. Harsh conditions are required, often including concentrated sulfuric acid and extremely high temperatures, to complete hydrolysis to a useful extent. In this work, the hydrolysis of cellulose was performed with acidic hydrogen molybdenum bronze in the form of XPell™ R by Xplosafe in place of sulfuric acid. By analyzing total organic carbon present in hydrolyzed samples (after 2 hours) using persulfate oxidation and colorimetric measurements, results were obtained showing that hydrogen molybdenum bronze is successful in catalyzing the hydrolysis of cellulose in comparison to hydrolysis completed in water alone. The values that were obtained in this analysis are as follows:  $160 \pm 20$  ppt/mol at 40 °C,  $180 \pm 20$  ppt/mol at 60 °C,  $180 \pm 30$  ppt/mol at 80 °C, and  $280 \pm 40$  ppt/mol at 100 °C. This determination shows that the catalytic ability of this acid increases with increasing temperature. Hydrogen molybdenum bronze is a useful candidate to explore in biofuel synthesis from cellulose. Comparison to sulfuric acid will be completed in future tests. This method is currently being used to pursue conversion of hydrolyzed cellulose to ethanol using yeast.

## ACKNOWLEDGEMENTS

To begin, I would like to express my deep appreciation for my research mentor, Dr. Dane W. Scott, for his knowledgeable and patient instruction during my undergraduate research. Dr. Scott's guidance and support were invaluable assets in this process, and I could not have had such a positive experience under different circumstances. I would also like to thank Dr. Reza Mohseni and Mr. Paul Tudico for taking time out of their extremely busy schedules to serve as readers of this thesis. Ultimately, I would also like to express my gratitude to East Tennessee State University, the ETSU Department of Chemistry, the ETSU Honors College, and the Honors-in-Discipline Scholarship Program for making every aspect of this research and my four years of undergraduate studies possible.

## LIST OF TABLES

Table	Page
I. Average absorbance values and calculated concentrations of TOC .....	23
II. TOC for all cellulose samples in ppm from calibration with KHP.....	24
III. TOC data calculated from the analysis of acid-hydrolyzed cellulose in terms of moles of $H_xMoO_3$ .....	24

## LIST OF FIGURES

Figure	Page
1. Representation of the sources of energy for consumption in the U.S., where petroleum, natural gas, and coal are all non-renewable fossil fuels.....	7
2. The truncated structure of cellulose which shows hydrogen bonding capabilities of the polymer. ....	10
3. Schematic representation of hydrogen spillover on tungsten (VI) oxide catalyzed by platinum. ....	13
4. The electronic structure of $H_xMoO_3$ ; white circles represent oxygen atoms and black circles represent molybdenum atoms in this dioctahedral structure. ....	14
5. Structure of the indicator molecule bromothymol blue .....	17
6. TOC spectrum obtained in this study with a maximum absorbance at 598.1 nm. ....	17
7. Calibration of TOC method by using sugar standards and determination of TOC in petroleum samples by calorimetric analysis. ....	19
8. Calibration curve generated for the TOC method with known standards of varying concentration of KHP. ....	22
9. TOC analysis of hydrolysis of cellulose at 40 °C, 60 °C, 80 °C, and 100 °C with XPell <sup>TM</sup> R expressed as ppt/mol. ....	25

## LIST OF SCHEMES

Scheme	Page
1. There are two possible hydrolytic products from the hydrolysis of cellulose into its constituent subunits: cellobiose and glucose. . . . .	11
2. Mechanism of carbonic acid formation in water . . . . .	16
3. Oxidation of hydrolysis products that gives detectable and quantifiable concentration of carbon dioxide with differing stoichiometric relationships for A) glucose and B) cellobiose. . . . .	18

## INTRODUCTION

In recent years, there has been an urgent push for the advancement of green chemistry and similar technology in light of the realization of human responsibility in environmental well-being. While green chemistry encompasses many areas and concerns in eco-friendly technology, this study will specifically focus on the issues related to the development of renewable fuels. Currently, the most widely used form of energy in the United States is provided by combustion of fossil fuels, which are considered to be a fuel source that is non-renewable. In 2015, 81% of the energy consumed by the U.S. was supplied by fossil fuel combustion.<sup>1</sup> Only 4.9% of the total energy consumption in this year was supplied by renewable biomass sources.<sup>1</sup> Biomass sources can include wood, food crops, grassy or woody plants, agricultural residues, algae, and organic components of industrial wastes.<sup>2</sup> The breakdown of this energy consumption is shown in Figure 1, where renewable sources include geothermal, solar, wind, hydroelectric, and biomass energy.<sup>1</sup>

U.S. Energy Consumption by Source (2015)

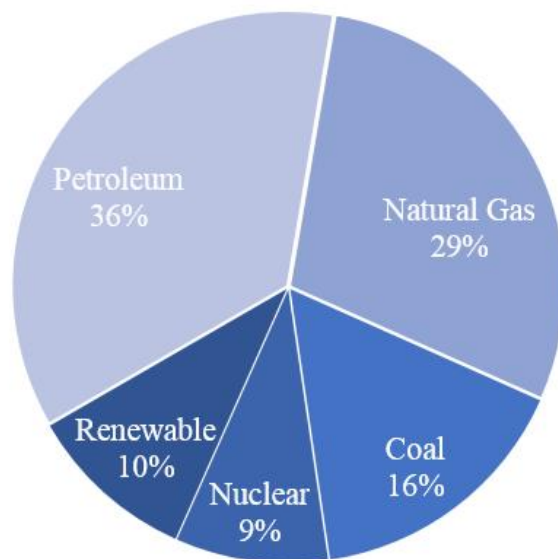


**Figure 1** – Representation of the sources of energy for consumption in the U.S., where petroleum, natural gas, and coal are all non-renewable fossil fuels.



## 6.1. NEED FOR BIOFUELS

Not only is the dependence on fossil fuels problematic due to these resources being limited and becoming rapidly exhausted, but they also contribute to climate change. Combustion of fossil fuels emits carbon dioxide, a greenhouse gas (GHG) that is one of the leading causes of climate change, into the atmosphere. Since the beginning of the Industrial Revolution, the concentration of atmospheric carbon dioxide has increased by more than 33%, leading to the conclusion that it is 95% probable that human activity has caused this increase.<sup>3</sup> While the combustion of cellulosic fuels does not eliminate the issue of carbon dioxide emission, the growth of cellulosic organisms removes carbon dioxide from the atmosphere via photosynthesis. Therefore, for a cellulosic fuel to be considered viable, U.S. Environmental Protection Agency (EPA) regulations require that it must provide a reduction in total GHG emission by 60% in comparison to fossil fuel emissions.<sup>4</sup>

The data shown in Figure 1 suggest that renewable biomass fuel sources are not among the major contributors to the energy consumed at this time and that there are current methods and technology in place for the production of biomass fuels. The two main processes are biochemically and thermochemically based.<sup>5</sup> Biochemical methods involve the use of enzymes and microorganisms as biocatalysts for the hydrolysis of cellulose. Thermochemical methods utilize heat and synthetic chemicals to catalyze hydrolytic reactions in cellulose molecules. In this study, hydrogen molybdenum bronzes ( $H_xMoO_3$ ) will be examined for their catalytic usefulness and efficacy in thermochemical conversion of cellulose to soluble products. Catalyzed hydrolysis is of interest because the abundant biomass cellulose can be converted into glucose as a precursor for a biofuel. This study will specifically address the issue of cellulose hydrolysis alone.

## 6.2. CELLULOSE AS AN ENERGY SOURCE

Ethanol has been utilized and developed in the fuel industry since the beginning of automotive travel in the late 19<sup>th</sup> century.<sup>6</sup> Today's methods of ethanol manufacturing include the conversion of starchy foods such as corn (contributes to over 95% of total ethanol production in U.S.), wheat, barley, etc. The use of crops in the production of ethanol has led to a debate over the concern for not only reducing the food supply directly by converting corn and grains to fuel, but also diverting the use of farmland to supplying crops for fuel rather than human sustenance. Cellulosic ethanol is produced from woody portions of trees, grasses, or plants; these materials are broken down into their component sugars which are then fermented to ethanol.<sup>6</sup>

Due to the absence of particular enzymes in human digestive systems, cellulose is inedible to humans and is, therefore, of much less concern in this food versus fuel dilemma. Additionally, cellulosic biofuels are often synthesized from materials such as the agricultural residue corn stover; the stalks, leaves, and husks of corn crops are not only inedible to humans, but they are also existing byproducts of current farming industry operations. Future predictions of the biomass fuel industry include more advanced energy crops which are fast-growing and grow in areas that do not support traditional agricultural crops.<sup>2</sup> These advantages over traditional ethanol production, in addition to the aforementioned ability of cellulosic materials to reduce overall GHG emission, have made cellulose particularly promising in the field of biofuel technology.

Structural stability in plant cells is predominantly provided by microfibrils of cellulose; it is this stability that introduces both advantages and major disadvantages in the production of cellulosic biofuels. The structure of crystalline cellulose is shown in Figure 2. This shows the extensive potential for hydrogen bonding on individual chains and adjacent chains of cellulose

polymers. Thermochemical hydrolysis of this organic polymer often requires the use of concentrated acids, high pressure environments, and extreme temperatures.<sup>7</sup> This is due to the extensive presence of inter- and intramolecular hydrogen bonding throughout the crystalline structure between glucose monomers and individual cellulosic chains; in addition, the presence of  $\beta(1\rightarrow4')$ -glycosidic linkages between D-glucose monomers contributes to the chemical stability and mechanical strength of cellulose.<sup>8</sup> The significance of this is that, by weight, crystalline cellulose provides more strength than steel, which makes hydrolysis difficult.<sup>9</sup>

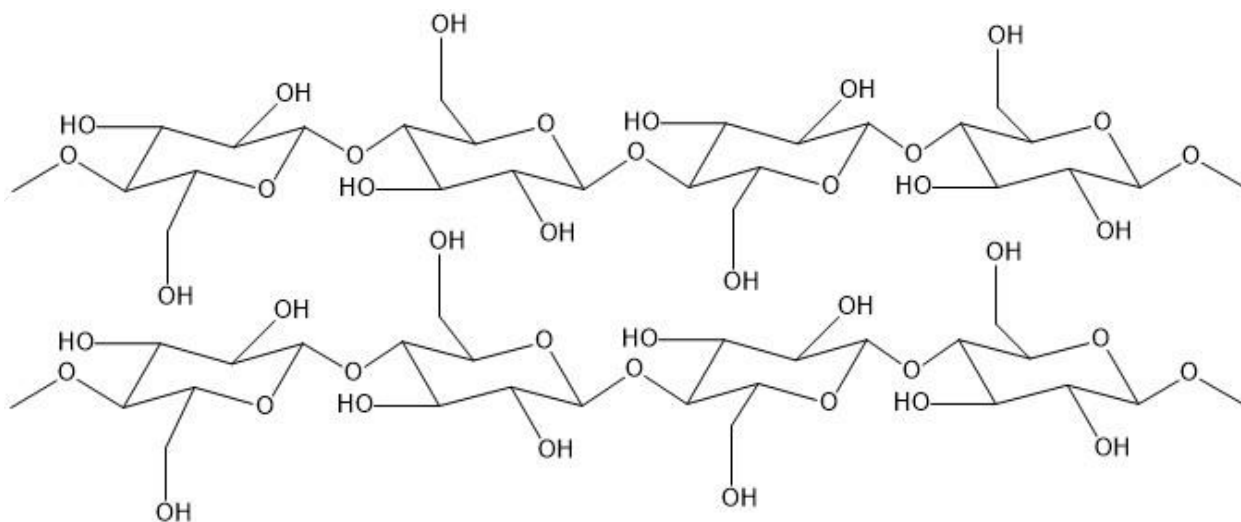
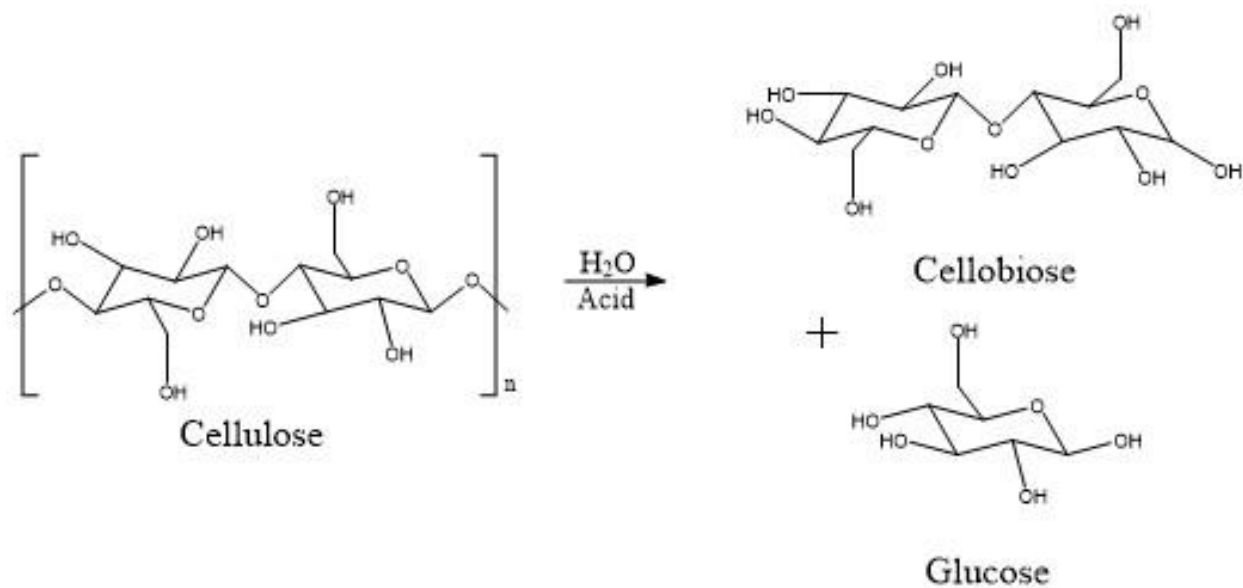


**Figure 2** – The truncated structure of cellulose which shows hydrogen bonding capabilities of the polymer.

Being a major structural component in the cells of all plant material, cellulose is the most abundant organic material on earth. Not only does this make cellulose readily available for current and future use, but it also ensures that the cost of acquisition of this precursor is fairly low.<sup>10</sup> The indeterminate length of these polymeric chains of cellulose makes hydrolysis impossible to determine without further experimentation. Hydrolysis could produce, for example, the disaccharide cellobiose; cellobiose is a disaccharide which consists of two  $\beta$ -glucose monomers and is soluble in water at ambient temperatures.<sup>11</sup> This issue can lead to ethanol yields from cellulose being low in some of these cellulosic fuel conversion processes if

the existence of cellobiose is not controlled or addressed. These two possible hydrolytic products are shown in Scheme 1. The acid that will be explored for its catalytic ability to produce simple sugars in this study is hydrogen molybdenum bronze.



**Scheme 1** – There are two possible hydrolytic products from the hydrolysis of cellulose into its constituent subunits: cellobiose and glucose.

### 6.3. HYDROGEN BRONZES FOR HYDROLYSIS OF CELLULOSE

Since the early 1970s, hydrogen bronzes have been analyzed for their ability to catalyze hydrogenation, reduction, and dehydration reactions.<sup>12</sup> These structures are useful for these types of catalysis due to the availability of hydrogen atoms on the surface of the material. One study found that even in the most reduced forms of  $H_xMoO_3$  (phase III,  $1.55 < x < 1.72$ ), hydrogen atoms occupy the outer, interlayer along zig-zag lines of the matrix rather than the intralayer spaces of the dioctahedral complex.<sup>12,13</sup> Additionally, the activation energy of hydrogen atom diffusion in  $H_xMoO_3$  is low, which creates variation in the stoichiometry of the material. The activation energies of the diffusion across these regions has been reported to be on the range of  $15 - 30 \text{ kJ mol}^{-1}$ .<sup>14</sup> These low activation energies do not only create more concentrated areas of hydrogen atoms in certain areas, but they also ensure that hydrogen atoms are available to participate in acidic catalysis.

Hydrogen bronzes in general (e.g.  $H_xMoO_3$ ,  $H_xV_2O_5$ , and  $H_xWO_3$ ) are most commonly prepared by hydrogen spillover, during which hydrogen molecules are dissociated into hydrogen atoms that deposited onto metal oxides in the presence of a precious metal catalyst.<sup>15</sup> A schematic of this mechanism of deposition on tungsten (VI) oxide is shown in Figure 3. It is expected that the mechanism of deposition on molybdenum (VI) oxide occurs in a similar fashion.

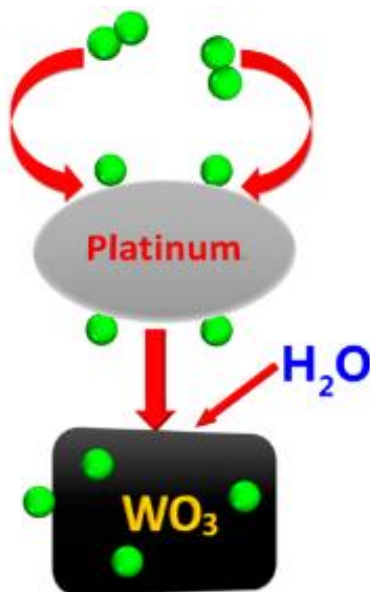


**Figure 3** – Schematic representation of hydrogen spillover on tungsten (VI) oxide catalyzed by platinum.<sup>16</sup>

Another efficient method that is often employed is the reduction of MoO<sub>3</sub> with Zn/HCl.<sup>13,17,18</sup> The most reduced phase of hydrogen molybdenum bronze, H<sub>2</sub>MoO<sub>3</sub>, can even be produced by reacting MoO<sub>3</sub> with Zn/HCl for a prolonged period.<sup>18</sup> These processes can take up to two weeks to complete, but this method has been shown to be successful in reducing metal oxides to hydrogen bronzes.<sup>17</sup> However, other methods of preparation exist, particularly for the preparation of hydrogen molybdenum bronzes.<sup>19,20</sup> The structure of the crystalline H<sub>x</sub>MoO<sub>3</sub> material has been determined to be orthorhombic with varying hydrogen concentrations diffusing across its surface;<sup>20</sup> an electronic representation of this structure, with the omission of hydrogen atoms on the surface, is shown below (Figure 4).

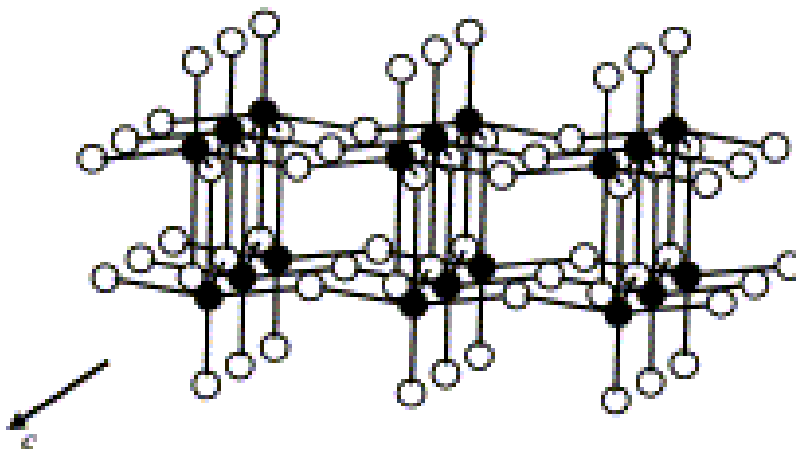


**Figure 4** – The electronic structure of  $H_xMoO_3$ ; white circles represent oxygen atoms and black circles represent molybdenum atoms in this dioctahedral structure.<sup>21</sup>

As mentioned before, hydrogen bronzes have been used as important materials in reduction, dehydration, and hydrogenation processes; recently,  $H_xMoO_3$  has also been studied for its potential utility as a functional component or conductive connection in nanowires, nanotubes, and nanobelts. This study focused on the ability of hydrogen molybdenum bronzes to provide mixed conductance from both protons and electrons in their orthorhombic matrix.<sup>22</sup> Hydrogen bronzes other than  $H_xMoO_3$ , namely, hydrogen vanadium bronze ( $H_xV_2O_5$ ) and hydrogen tungsten bronze ( $H_xWO_3$ ) can be prepared for similar reactions and catalytic purposes via similar methods. Hydrogen spillover in  $MoO_3$  occurs much faster than hydrogen spillover in  $WO_3$ , however,<sup>16</sup> often making it less expensive and more accessible for utilization of its catalytic ability in many cases.

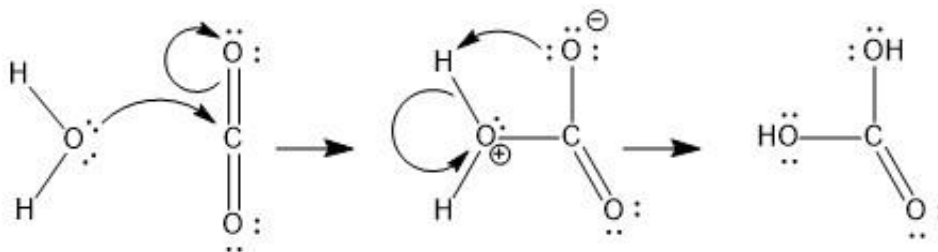
Hydrogen molybdenum bronzes ( $H_xMoO_3$ , where  $0 < x \leq 2$ )<sup>22</sup> have metallic bond character and exhibit conductive properties, whereas molybdenum oxides are semiconductive prior to introduction of hydrogen.<sup>23</sup> When hydrogen is introduced to a  $MoO_3$  system, hydrogen bonding occurs on the exterior oxygen atoms of the  $MoO_3$  system; the low activation energy needed for these protons to diffuse across the surface to other oxygen atoms creates variation in

the stoichiometry of the system.<sup>23</sup> Studies have shown that the nonstoichiometric forms of  $H_xMoO_3$  can be categorized as follows:  $H_{0.23-0.40}MoO_3$  is blue (orthorhombic),  $H_{0.85-1.04}MoO_3$  is blue (monoclinic),  $H_{1.55-1.72}MoO_3$  is red, and  $H_2MoO_3$  is green.<sup>23</sup> The form that will be used in this study (XPell<sup>®</sup> R by Xplosafe, LLC) is dark blue in color, indicating that it is one of the lower integer stoichiometric forms. This compound has been used to carry out hydrolysis of cellulose and the amount of products were determined by total organic carbon (TOC) analysis.



#### 6.4. TOTAL ORGANIC CARBON DETERMINATION OF HYDROLYZED CELLULOSE

Total organic carbon analyses have several useful applications that have been utilized effectively for over a decade in both industrial and environmental chemistry. These applications include, but are not limited to: water contamination, characterization of samples, and determination of soil carbon content.<sup>24</sup> The basis of these determinations is the oxidation of TOC to carbon dioxide which is absorbed by the indicator solution resulting in a color change due to the formation of carbonic acid. This reaction occurs between dissolved carbon dioxide and water, where water acts as a nucleophile and carbon dioxide acts as the substrate. Proton transfer from water to oxygen in carbon dioxide then generates carbonic acid. This mechanism is shown in Scheme 2.



**Scheme 2** – Mechanism of carbonic acid formation in water

In this study, bromothymol blue will serve as the indicator and will change to the yellow form in acidic solution. The structure of bromothymol blue is shown below in Figure 5, where the basic form is on the right and the acidic form is on the left. The change in absorbance can be measured using a simple Vernier spectrophotometer. A sample spectrum obtained in this study is shown below in Figure 6. The wavelength of maximum absorbance is 598.1 nm.

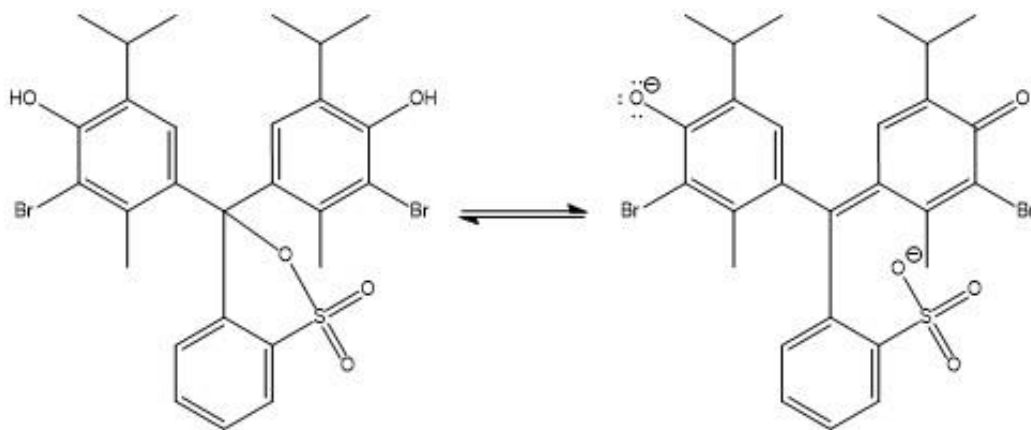


**Figure 5** – Structure of the indicator molecule bromothymol blue

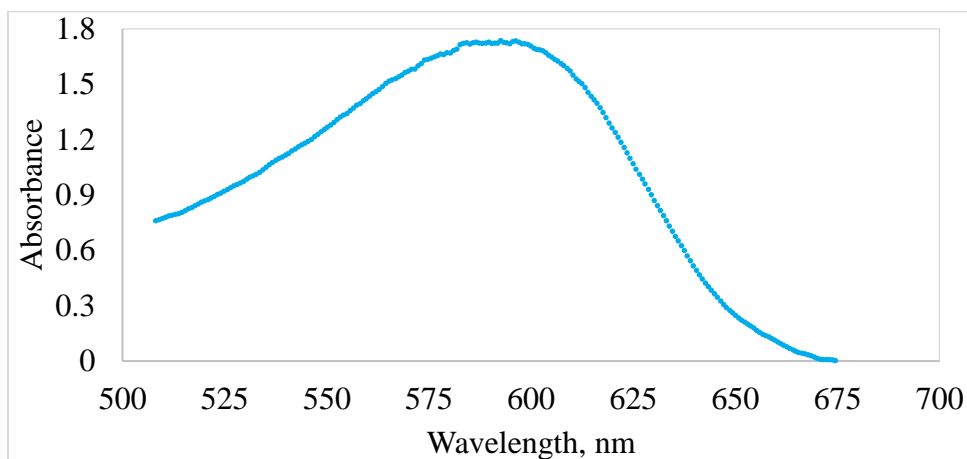
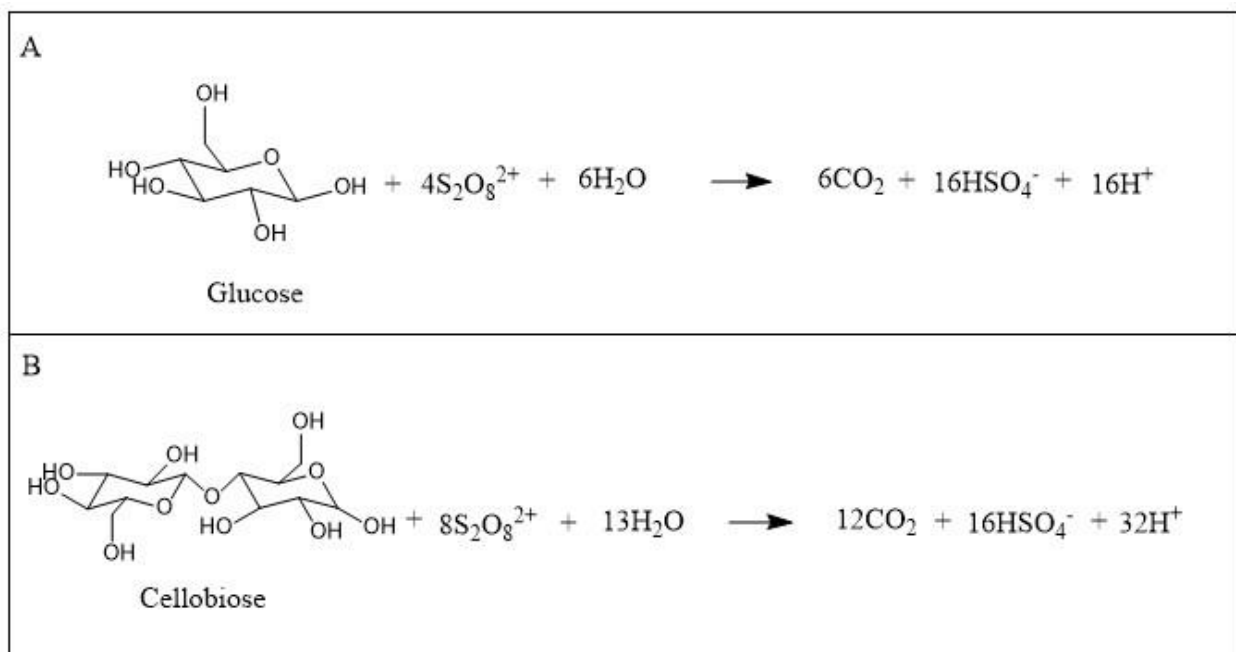


**Figure 6** – TOC spectrum obtained in this study with a maximum absorbance at 598.1 nm.

In real samples, there are considerations and corrections that must be made for interference in measurement from inorganic carbon and trace metals for TOC analysis. However, for this study, samples will be prepared to contain organic carbon only. The existence of these interferences will be addressed by finding the difference of absorbance values between blank samples (cellulose and water) and catalyzed samples (cellulose,  $H_xMoO_3$ , and water) under identical conditions.

There are two common methods of oxidation used to achieve these measurements of carbon dioxide concentration: combustion and chemical oxidation. Combustion methods

introduce more problematic interferences from inorganic carbon.<sup>24</sup> Chemical oxidation, which is the method utilized in this study, can be accomplished with varying oxidant strengths according to the needs and specifications of the analysis. Examples of these oxidants include potassium dichromate in sulfuric acid, silver (I) sulfate, phosphoric acid, and persulfate ( $K_2S_2O_8$ ); use of these methods is most often optimal for soils and sediments, while the use of persulfate is utilized more frequently in determination of organic carbon that is dissolved in aqueous solutions without inorganic carbon present (or by removing it).<sup>24</sup> These oxidative reactions must be accompanied by the addition of energy in the form of heat or ultraviolet radiation. These reactions take place according to the equation shown in Scheme 3.



**Scheme 3** – Oxidation of hydrolysis products that gives detectable and quantifiable concentration of carbon dioxide with differing stoichiometric relationships for A) glucose and B) cellobiose.

Determination of TOC is an important method in that it can be performed simply and quickly on a wide variety of samples in small sample sizes to provide sensitive measurements of low detection limits. Some reported detection limits as low as  $10^{-3}$  mM dissolved TOC.<sup>25</sup> Linear

responses are expected and can be verified with standards of organic molecules. An example of the type of data that can be obtained from these analyses is shown in Figure 7; this study used TOC to determine hydrocarbon contamination of soil by comparing unknown samples to a calibration curve of known sugar samples.<sup>26</sup> Similar linear responses were obtained in this study. One important limitation of this method, however, is the ambiguity that exists in the results that are obtained. As long as a substance contains carbon and is oxidizable, then it will be detected as carbon dioxide by this technique.<sup>25</sup> This suggests that any dissolved forms of hydrolyzed cellulose, whether they are glucose molecules, cellobiose molecules, or larger molecules, will contribute to the amount of TOC measured.

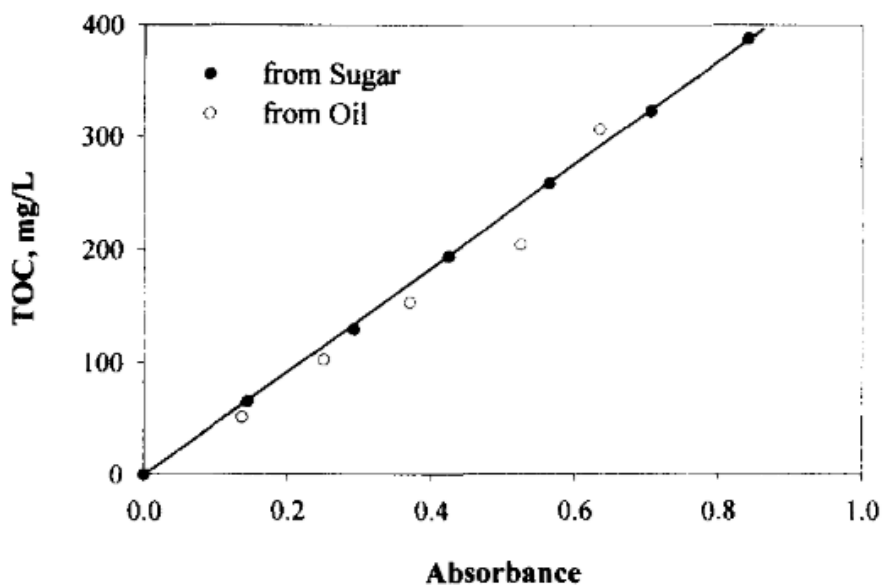


**Figure 7** – Calibration of TOC method by using sugar standards and determination of TOC in petroleum samples by calorimetric analysis.<sup>26</sup>

## EXPERIMENTAL

### 7.1. MATERIALS AND METHODS

All trials were performed with commercially isolated and purified microcrystalline cellulose. Other reagents utilized in this work were also obtained from commercial sources and were utilized in their original forms without further alteration. These materials include: XPell™ R (>99.5% MoO<sub>3</sub> and <0.5% proprietary blend) by Xplosafe, LLC; potassium hydrogen phthalate (KHP); 18 MΩ water; and the Hach TOC (total organic carbon) Test Kit, Low Range, 0-20 mg/L reagent set (Mfr #27603-45). Techniques used in this study include the hydrolysis of cellulose by digestion in water with XPell™ R, conversion of TOC to carbon dioxide by persulfate oxidation with digestion, and spectroscopic analysis of carbonic acid in an indicator solution. This TOC method was calibrated with potassium hydrogen phosphate (KHP). These hydrolytic and spectroscopic methods were measured and analyzed with the following instrumentation and data analyzing software: Metler Toledo precision balance ML203T/00; Vernier SpectroVis® Plus spectrophotometer; Hach DRB200 Dry Thermostat Reactor Block for TNTplus (DRB200-03); Vernier LabQuest® Mini; Logger Pro 3 software; and Sorvall™ Legend™ XT Centrifuge. Spectroscopic values of absorption were recorded at  $\lambda_{\text{max}}$  (598.1 nm).

### 7.2. EXPERIMENTAL PROCEDURE

The Hach DRB200 reactor instrument was calibrated for detection of TOC with 200 mL solutions of 2, 4, 6, 8, 10, and 20 ppm KHP and a reagent blank (deionized water in absence of KHP). This was conducted by using these KHP samples in the procedure provided by Hach.<sup>27</sup> This process included stirring a solution of 10 mL of the sample solution with 0.4 mL of a buffer solution with a pH of 2.00 for 10 minutes. For each KHP standard solution, 3.00 mL were then placed in a vial with a premeasured amount of persulfate (white powder) was added with glass

indicator ampules (bromothymol blue). These vials were capped and heated in the DRB200 instrument at 105 °C for 2 hours. After cooling these samples for at least 1 hour, the indicator solution was analyzed in the SpectroVis<sup>®</sup> Plus instrument via Logger *Pro* 3 software. It was determined that the  $\lambda_{\text{max}}$  for this analysis was 598.1 nm, which agrees with the reported  $\lambda_{\text{max}}$  by the Hach TOC method.<sup>27</sup> Absorbance values were recorded at this wavelength.

After calibration, microcrystalline cellulose was hydrolyzed. Hydrolysis was carried out by placing approximately 0.1 g of microcrystalline cellulose in an empty, clean TOC vial with approximately 1.00 mmol of acid catalyst, XPell<sup>™</sup> R, and 4 mL of water. The exact masses of XPell<sup>™</sup> R added were recorded as they were measured. The molar mass of  $\text{H}_x\text{MoO}_3$  (the value of  $x$  is proprietary) was assumed to be the maximum possible value for purposes of calculations, where  $x = 2$  (MM = 145.95 g/mol). Triplicate trials of hydrolysis were carried out for two hours at 40 °C, 60 °C, 80 °C, and 100 °C. These solutions were centrifuged. The supernatant was decanted and the solids were washed and centrifuged three times. The color of the supernatant changed from an original color of dark blue from soluble XPell<sup>™</sup> R to clear. These solutions were diluted to 200 mL using deionized water in a volumetric flask. These diluted samples were analyzed with the previously described TOC method and values of absorption were recorded. The calibration curve generated from TOC analysis of KHP standard solutions was used to calculate total organic carbon concentrations and uncertainty.

## RESULTS AND DISCUSSION

### 8.1. CALIBRATION OF TOC METHOD

Calibration of the method for TOC analysis is shown below in Figure 8.

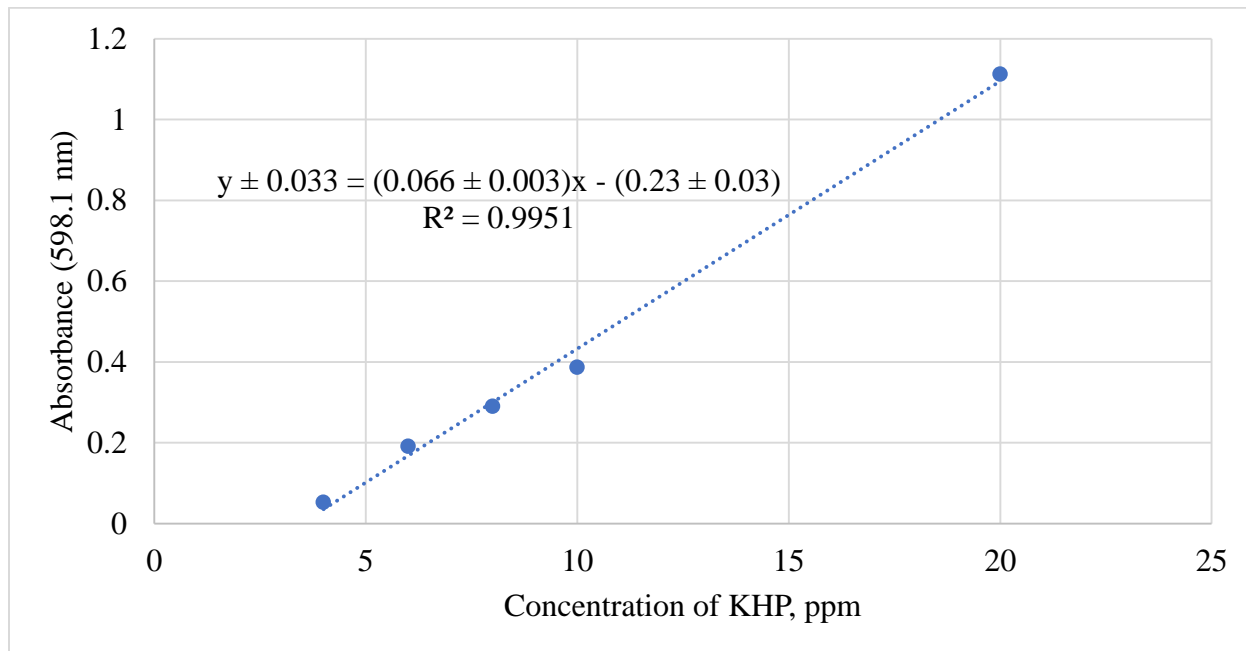


**Figure 8** - Calibration curve generated for the TOC method with known standards of varying concentration of KHP.

The equation of the line in Figure 8 was then used as the basis for calculating the concentrations of TOC in all samples. As the correlation coefficient of 0.9951 suggests, the method produces a reliable linear response.

### 8.2. AVERAGE ABSORBANCES AND TOC CONCENTRATIONS

The average absorbance values for each trial were recorded for each of the hydrolyzed cellulose samples. These values are shown in Table I.

**Table I** – Average absorbance values and calculated concentrations of TOC

Temperature	Average Sample Absorbance Measurement	Average Blank Absorbance Measurement
40 °C	1.680	1.667
60 °C	1.674	1.682
80 °C	1.630	1.652
100 °C	1.663	1.817

As shown in Table I, the absorbance values obtained for the blank samples were often higher than those obtained for the catalyzed samples and generally increased with increasing temperature. This is due to the nature of the indicator and technique utilized in this determination. A decrease in absorbance at a wavelength of 598.1 nm indicates an increase in the yellow (acidic) form of bromothymol blue and a higher concentration of CO<sub>2</sub>. Because hydrolysis of cellulose occurs in water only (blank samples), these absorbance values are not expected to be constant as temperature changes. As such, an increase in the absorbance difference between the blank and samples hydrolyzed with hydrogen molybdenum bronze increases with temperature.

Using these absorbance values and the calibration curve determined in Figure 8, TOC and respective uncertainty values were calculated. Examples of these calculations for the 40 °C trials are shown in Equation 1.

$$y \pm 0.033 = (0.066 \pm 0.003)x - (0.23 \pm 0.03)$$

$$x = \frac{(-0.013 \pm 1.96\%) + (0.23 \pm 13.0\%)}{(0.066 \pm 4.55\%)}$$

$$x = 3.3 \pm 0.4 \text{ ppm}$$

(1)



These values for each trial are shown in Table II.

**Table II** – TOC for all cellulose samples in ppm from calibration with KHP

Temperature	Average Calculated TOC Concentration (ppm)
40 °C	3.3 ± 0.4
60 °C	3.6 ± 0.5
80 °C	3.8 ± 0.5
100 °C	5.8 ± 0.8

The average relative uncertainty in these values was approximately 13.8%; this was due mostly to the calculated error in the y-intercept value from the equation in Figure 8. The values of the original, concentrated sample TOC concentrations in each temperature trial were then determined by accounting for dilutions and converted to units of ppt (parts per thousand) from ppm. In order to evaluate the efficacy of the catalyst at these temperatures, TOC is expressed per mole of catalyst used. These values obtained from this analysis are shown in Table III.

**Table III** – TOC data calculated from the analysis of acid-hydrolyzed cellulose in terms of moles of  $H_xMoO_3$

Temperature	ppt TOC/mole of catalyst
40 °C	160 ± 20
60 °C	180 ± 20
80 °C	180 ± 30
100 °C	280 ± 40

These data were calculated with an average relative uncertainty of 14.0% due to the aforementioned error in the y-intercept value and the uncertainty in the dilution factor that was

used to determine the concentration in the original samples. While the 40 °C, 60 °C, and 80 °C trials showed little change in TOC concentration within error of one another, the 100 °C trial displayed a statistically significant increase in the concentration of TOC. Figure 9 shows the amount of TOC in ppt/mol XPell™ as a function of temperature.

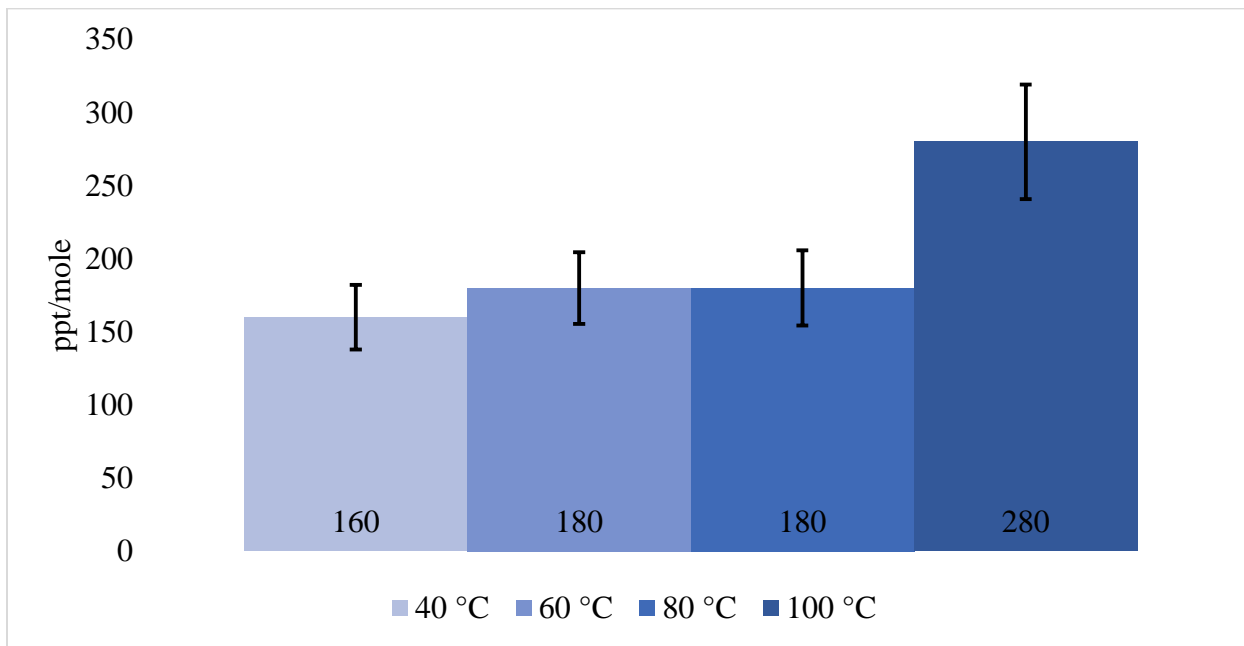


**Figure 9** - TOC analysis of hydrolysis of cellulose at 40 °C, 60 °C, 80 °C, and 100 °C with XPell™ R expressed as ppt/mol.

## CONCLUSIONS

In this study, it was shown that hydrogen molybdenum bronze catalyzes hydrolysis of microcrystalline cellulose. The concentration of TOC increases with temperature. This was successfully determined by using the method of total organic carbon analysis with persulfate oxidation of organic carbon in an aqueous sample. Specifically, temperature trials of hydrolyzing microcrystalline cellulose at 40 °C, 60 °C, and 80 °C showed slight but relatively insignificant increases in TOC concentrations per mole of  $H_xMoO_3$ , which were  $160 \pm 20$  ppt/mol,  $180 \pm 20$  ppt/mol, and  $180 \pm 30$  ppt/mol, respectively. The trial at 100 °C did show a significant increase in TOC per mole over the 80 °C trial at a value of  $280 \pm 40$  ppt/mol.

The TOC method was calibrated in this work with pure KHP. The obtained calibration curve exhibited low detection limits, sensitivity, and a strong linear correlation ( $R^2 = 0.9951$ ) which was expected of the method. The absorbance values that were obtained for the blank samples generally showed an increase in absorbance while the absorbance values of the catalyzed samples decreased slightly. The difference in absorbance between these values shows that hydrolysis with a catalyst increased in comparison to simple hydrolysis with increasing temperature.

While some uncertainty was obtained in these measurements, the calculated amount of TOC per mole of  $H_xMoO_3$  showed a measureable increase with temperature over all trials. The limitation of TOC analysis ambiguity was not overcome in this study; the extent of hydrolysis and the identity of the products (glucose, cellobiose, etc.) was not determined. Due to the presence of this variable, the exact percent of cellulose that was hydrolyzed is unknown. The ability of the measurements to provide information regarding an observable concentration of organic carbon in the hydrolyzed samples, however, shows that hydrolysis is possible under

these relatively mild conditions. This study ultimately showed the utility of acid-catalyzed hydrolysis of cellulose with  $H_xMoO_3$  for the purpose of biofuel synthesis.

## FUTURE PROSPECTS

In order for this method to be a viable option in acid pretreatment of cellulose for biofuel synthesis, the catalyst must be removed from the reaction system before the next synthetic step takes place. XPell™ R is a fine, powdery material that is soluble in water. These physical characteristics will create difficulty in separating it from the aqueous solution; its dark blue color, however, will provide a manner of detection for its removal. Additionally, the efficiency of this catalysis method will be compared to the catalyzed hydrolysis of cellulose by both sulfuric acid and phosphomolybdic acid to determine the most efficacious acid using similar conditions. Further research is currently being performed to determine the identity of the products of hydrolysis and their relative concentrations. These products could be separated and quantified by HPLC. Another area of research is currently being pursued with Dr. Steven Fields using the hydrolyzed cellulose solution and making an agar plate for fermentation by isolated yeast strains and quantifying the products.

## REFERENCES

---

1. U.S. Energy Information Administration: Energy Explained: U.S. Energy Facts: Nonrenewable Sources. [https://www.eia.gov/EnergyExplained/?page=us\\_energy\\_home](https://www.eia.gov/EnergyExplained/?page=us_energy_home) (accessed Feb 1, 2017).
2. National Renewable Energy Laboratory: Working with Us: Biomass Energy Basics. <https://www.nrel.gov/workingwithus/re-biomass.html> (accessed Feb 15, 2017).
3. NASA. Climate Change: Vital Signs of the Planet: Causes. <http://climate.nasa.gov/causes/> (accessed Feb 15, 2017).
4. EPA. Renewable Fuel Standard Program: Program Overview. **2016**, <https://www.epa.gov/renewable-fuel-standard-program/> (accessed Feb 15, 2017).
5. U.S. Department of Energy: Biofuel Conversion Basics. <https://energy.gov/eere/energybasics/articles/biofuel-conversion-basics> (accessed Feb 15, 2017).
6. Solomon, B. D.; Barnes, J. R.; Halvorsen, K. E. Grain and cellulosic ethanol: History, economics, and energy policy. *Biomass Bioenergy* **2007**, *31* (6), 416-425.
7. Suib, S. L. *New and Future Developments in Catalysis: Catalytic Biomass Conversion*. Elsevier: Amsterdam, **2013**.
8. Agoda-Tandjawa, G.; Durand, S.; Gaillard, C.; Garnier, C.; Doublier, J. L. Properties of cellulose/pectins composites: Implication for structural and mechanical properties of cell wall. *Carbohydr. Polym.* **2012**, *90* (2), 1081-1091.
9. Altaner, C. M.; Thomas, L. H.; Feranades, A. N.; Jarvis, M. C. How Cellulose Stretches: Synergism between Covalent and Hydrogen Bonding. *Biomacromolecules*, **2014**, *15* (3), 791–798.

- 
10. Lynd, L. R.; Weimer, P. J.; van Zyl, W. H.; Pretorius, I. S. Microbial Cellulose Utilization: Fundamentals and Biotechnology. *Microbiol. Mol. Biol. Rev.* **2002**, *66* (3), 506–577.
  11. Hu, L.; Lin, L.; Wu, Z.; Zhou, S.; Liu, S. Chemocatalytic hydrolysis of cellulose into glucose over solid acid catalysts. *Appl. Catal., B* **2015**, *174-175*, 225-243.
  12. Yang, M.; Han, B.; Cheng, H. First-Principles Study of Hydrogenation of Ethylene on a  $H_xMoO_3(010)$  Surface. *J. Phys. Chem. C* **2012**, *116*, 24630-24638.
  13. Braïda, B.; Adams, S.; Canadell, E. Concerning the Structure of Hydrogen Molybdenum Bronze Phase III. A Combined Theoretical-Experimental Study. *Chem. Mater.* **2005**, *17*, 5957-5969.
  14. Ritter, C.; Müller-Warmuth, W.; Schöllhorn, R. Structure and motion of hydrogen in molybdenum bronzes  $H_xMoO_3$  as studied by nuclear magnetic resonance. *J. Chem. Phys.* **1985**, *83* (12), 6130-6138.
  15. Chen, L.; Cooper, A. C.; Pez, G. P.; Cheng, H. On the Mechanisms of Hydrogen Spillover in  $MoO_3$ . *J. Phys. Chem. C* [Online] **2008**, *112*, 1755-1758.
  16. Xi, Y.; Zhang, Q.; Cheng, H. Mechanism of Hydrogen Spillover on  $WO_3(001)$  and Formation of  $H_xWO_3$  ( $x = 0.125, 0.25, 0.375, \text{ and } 0.5$ ). *J. Phys. Chem. C* [Online] **2014**, *118*, 494-501.
  17. Crouch-Baker, S.; Dickens, P. G. Hydrogen Insertion Compounds of the Molybdic Acids,  $MoO_3 \cdot nH_2O$  ( $n=1,2$ ). *Mat. Res. Bull.* **1984**, *19*, 1457-1462.
  18. Birtill, J. J.; Dickens, P. G. Phase Relationships in the System  $H_xMoO_3$  ( $0 < x \leq 2$ ). *Mat. Res. Bull.* **1978**, *13*, 311-316.

- 
19. Noh, H.; Wang, S.; Luo, S.; Flanagan, T. B.; Balasurbramaniam, R.; Sakamoto, Y. Hydrogen Bronze Formation within Pd/MoO<sub>3</sub> Composites. *J. Phys. Chem. B* [Online] **2004**, *108*, 310-319.
20. Zhou, C. X.; Wang, Y. X.; Yang, L. Q.; Lin, J. H. Syntheses of Hydrated Molybdenum Bronzes by Reduction of MoO<sub>3</sub> with NaBH<sub>4</sub>. *Inorg. Chem.* [Online] **2001**, *40*, 1521-1526.
21. Scherlis, D. A.; Lee, Y. J.; Rovira, C.; Adams, S.; Nieminen, R. M.; Ordejón, P.; Canadell, E. Concerning the origin of superstructures in hydrogen molybdenum bronzes H<sub>x</sub>MoO<sub>3</sub>. *Solid State Ionics* **2004**, *168*, 291-298.
22. Hu, X. K.; Qian, Y. T.; Song, Z. T.; Huang, J. R.; Cao, R.; Xiao, J. Q. Comparative Study on MoO<sub>3</sub> and H<sub>x</sub>MoO<sub>3</sub> Nanobelts: Structure and Electric Transport. *Chem. Mater.* [Online] **2008**, *20*, 1527-1533.
23. Sha, X.; Chen, L.; Cooper, A. C.; Pez, G. P.; Cheng, H. Hydrogen Absorption and Diffusion in Bulk α-MoO<sub>3</sub>. *J. Phys. Chem. C* [Online] **2009**, *113*, 11399-11407.
24. Bisutti, I.; Hilke, I.; Raessler, M. Determination of total organic carbon – an overview of current methods. *Trends Anal. Chem.* **2004**, *23*, 716-726.
25. Kfoury, M.; Auezova, I.; Greige-Gerges, H.; Fourmentin, S. Development of a Total Organic Carbon method for the quantitative determination of solubility enhancement by cyclodextrins: Application to essential oils. *Anal. Chim. Acta* **2016**, *918*, 21-25.
26. Schreier, C. G.; Walker, W. J.; Burns, J.; Wilkenfeld, R. Total Organic Carbon as a Screening Method for Petroleum Hydrocarbons. *Chemosphere* **1999**, *39* (3), 503-510.
27. Hach DRB200: Digital Reactor Block: 15 x 16 mm vial wells, 230 Vac: Parameter/Reagent: Total Organic Carbon: 10129 DR800, LR Direct. <https://www.hach.com/asset-get.download.jsa?id=7639983636> (accessed Feb 1, 2016).